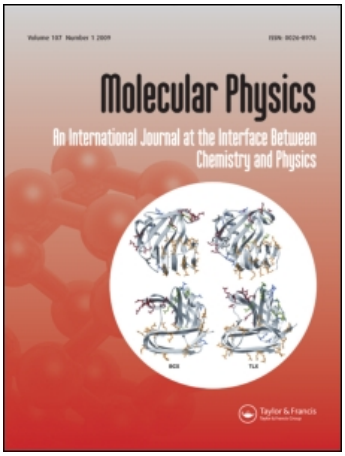

Molecular Physics
Publication details, including instructions for authors and subscription information:
http://www.informaworld.com/smpp/title~content=t713395160

Effect of water-methanol content on the structure of Nafion in the sandwich model and solvent dynamics in nano-channels; a molecular dynamics study

Hadi Abroshan[a]; Hamed Akbarzadeh[a]; Farid Taherkhani[b]; Gholamabbas Parsafar[ac]
[a] Department of Chemistry, Sharif University of Technology, Tehran, Iran [b] Department of Chemistry, Razi University, Kermanshah, Iran [c] Nanotechnology Research Center, Sharif University of Technology, Tehran, Iran

Online publication date: 03 March 2011

To cite this Article Abroshan, Hadi , Akbarzadeh, Hamed , Taherkhani, Farid and Parsafar, Gholamabbas(2011) 'Effect of water-methanol content on the structure of Nafion in the sandwich model and solvent dynamics in nano-channels; a molecular dynamics study', Molecular Physics, 109: 5, 709 — 724
To link to this Article: DOI: 10.1080/00268976.2010.549846
URL: http://dx.doi.org/10.1080/00268976.2010.549846

Molecular Physics
Vol. 109, No. 5, 10 March 2011, 709–724

Taylor & Francis
Taylor & Francis Group

RESEARCH ARTICLE

Effect of water–methanol content on the structure of Nafion in the sandwich model and solvent dynamics in nano-channels: a molecular dynamics study

Hadi Abroshan[a], Hamed Akbarzadeh[a], Farid Taherkhani[b] and Gholamabbas Parsafar[ac]*

[a]*Department of Chemistry, Sharif University of Technology, Tehran, Iran;* [b]*Department of Chemistry, Razi University, Kermanshah, Iran;* [c]*Nanotechnology Research Center, Sharif University of Technology, Tehran, Iran*

(*Received 18 October 2010; final version received 15 December 2010*)

Continuing an ongoing study, molecular dynamics (MD) simulations were performed to investigate the effects of methanol concentration on Nafion morphology, such as the size of solvent cluster, solvent location, and polymer structure via the sandwich model. Our survey shows that high methanol concentrations resulted in increment of solvent cluster size in Nafion membrane. The sulfonic acid clusters also befall much in order as subsequent layers of such ionic clusters are formed. The number of neighbouring hydronium ions around a sulfur atom is independent of methanol concentration, but the first shell of hydronium and water around sulfonic acid clusters is broader. Although methanol would prefer to interact with water molecules rather than sulfonic acid groups, gathering of methanol molecules via hydrophobic self-aggregation is preferred. Methanol is located closer to the hydrophobic part of the polymer than water, while water is located closer to the hydrophilic part of the polymer. It was found that methanol distributes specifically more than water in nano-channels. Investigation of solvent dynamics in nano-channels shows that diffusion coefficients (D) of water, methanol, and hydronium decrease with increasing methanol concentration and they may be ordered as follows: $D_{\mathrm{Water}} > D_{\mathrm{Methanol}} > D_{\mathrm{Hydronium}}$ ($D_{\mathrm{Water}} \approx 1.6$–$2.0 D_{\mathrm{Methanol}}$ and $D_{\mathrm{Methanol}} \approx 2.1$–$3.0 D_{\mathrm{Hydronium}}$).

Keywords: proton exchange membrane; Nafion; Sandwich Model; nano-channels; molecular dynamics simulation

1. Introduction

Ion-conducting polymer membranes are a focus of materials science nowadays due to their potential applications in environment-friendly energy sources, i.e. fuel cells suitable for electronic equipments, medical devices and electric vehicles [1–7]. A special group of these materials are the proton exchange membranes (PEM), which have promising applications in electrochemical devices [8,9]. Novel PEMs that possess good chemical and mechanical stability, low gas permeability, and high proton conductivity are needed, and the route to successful implementation of these power sources requires a systematic understanding of how proton mobility is determined by the polymer structure and chemistry, water, methanol, and water/methanol contents, and choice of the pendant group.

Nafion is a poly-tetrafluoroethylene polymer with hydrophilic perfluorovinyl pendant side chains terminated with sulfonic acid groups (Figure 1), used as a proton-conducting membrane in methanol and oxygen–hydrogen fuel cells. Nafion's structure, characterized by a microphase separation, has been widely studied using small angle neutron scattering (SANS) or small angle X-ray scattering (SAXS) [10–15]. Various models have emerged to explain the properties of hydrated Nafion membrane. For a review of different models proposed for Nafion see Ref. 16. Central to each different proposed model is the recognition that the ionic groups aggregate in the perfluorinated polymer matrix to form a network of clusters that allow for significant swelling by polar solvents and efficient ionic transport through these nanometre-scale domains. These models, however, differ significantly in the geometry and spatial distribution of the ionic clusters [16]. Most studies show that the microstructure of Nafion consists of three regions: hydrophobic fluorocarbon backbone, hydrophilic ionic clusters of sulfonic acid groups, and interfacial regions. In many investigations, formation of inverted micelles in the Nafion structure has been proposed. In such proposals, the hydrophilic ionic clusters of sulfonic acid groups along with water molecules present in the Nafion membrane interact with each other. At the same time, hydrophobic fluorocarbon backbones interact with each other as well [11,17–26]. The sandwich-like model, which was proposed by Haubold *et al.* is a model with discrete

*Corresponding author. Email: parsafar@sharif.edu

ISSN 0026–8976 print/ISSN 1362–3028 online

DOI: 10.1080/00268976.2010.549846
http://www.informaworld.com

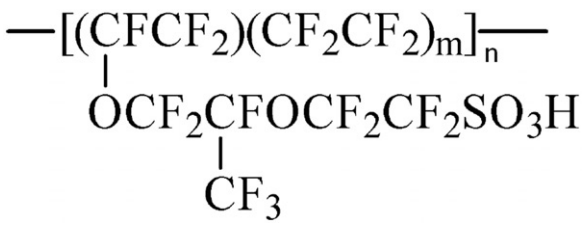

Figure 1. Chemical formula of Nafion with two parameters; m and n.

sandwich-like structure elements for the nano-structure of the cross-linked channel system within the membrane [24]. This model consists of a shell region and an embedded core region, the latter region being either empty or flooded by water and methanol. They proposed that the complex structure of the cross-linked channels can be described by a composition of these basic structure elements (see Figures 6 and 7 of Ref. 24), and assumed that they are randomly distributed inside the volume of the membrane. In summary, the scattering data indicates that this simple structural model is able to describe the swelling behaviour of Nafion on a nanometre scale [24]. Of the different models proposed for Nafion, Ryu *et al*. believe that those of Gierke *et al*. and Haubold *et al*. most lucidly model the relationship between Nafion structure and the hydronium transport phenomenon [25]. Elfring *et al*. suggested that since the transport through bulk water presents an upper limit for protonic conductivity, it is important to determine the permeation of the liquid phase and its connectivity in order to quantify the various modes of proton transport. The morphological models mentioned before are wide ranging [26]. They tended to favour the interpretation given by Kreuer [27], which is reflected in the AFM imaging conducted by McLean *et al*. [28]. They concluded that the morphological models which present more order, such as the cluster network model or the 'sandwich' structured model, are distillations of such an interpretation [26].

In the direct methanol fuel cell (DMFC) system, the water path causes methanol transport through the membrane to the cathode, known as methanol crossover. This phenomenon is one of the serious problems for the practical application of the membranes to the DMFC technology because it is responsible for fuel loss and cell potential reduction due to mixed potential at the cathode. The problem is accelerated by higher methanol concentration of solution. Computer simulations of Nafion membrane in water/methanol solvent by Chertovich *et al*. have shown that the conductivity parameter in Nafion is strongly dependent on the solvent composition and determined by the solvation effects and the spatial distribution of polar sulfonate groups in ion-conductive channels [29]. An understanding of the morphology of the membranes swelling in methanol or in water/methanol mixture is thus a key factor for DMFC development. Fundamental characterizations of the structure of the membrane and its relationship to proton and small molecular transport is needed to gain a more thorough understanding of performance, stability, and degradation, and to tailor membranes that meet the demands of fuel cell applications [30–34].

Molecular dynamics (MD) simulation has been proven to be the most helpful tool to complement experimental studies. MD techniques are especially appropriate for studying complex polymer systems, since it can be used to expose nano-structure features with or without assuming any priori specific structural model [35–38]. There are some theoretical investigations of the membranes solvated in water, methanol, and water/methanol mixtures as well as water-, methanol-, and water/methanol mixtures-swollen membranes [34,39–42]. In previous work [43] we presented results of the dynamical behaviour of solvent and its dependence on Nafion polymerization and structure, considering the sandwich model. It has been shown how distances among sulfonic acid groups can affect structure of the sandwich model components and arrangements as well as water and hydronium diffusion coefficients. In the current study, we particularly explore the effects of level of water–methanol content on the structure of Nafion throughout the sandwich model by means of classical molecular dynamics simulations. As we especially focus our attention on methanol concentration dependence of the membrane morphology, we have carried out a series of MD simulations for Nafion membranes swelling in solutions with six different methanol concentrations. Water, methanol, and hydronium dynamics in nanochannels of the sandwich model are also analysed and discussed as a function of methanol concentration.

2. Method

2.1. *Set of systems*

Six types of Nafion membrane, differing in the water/methanol ratio content, with respect to the sandwich model were produced for simulations. In all systems the value of parameters m and n (for definition of m and n, see Figure 1) are taken to be 7 and 9, respectively. The initial coordination of each system was obtained as follows. One unit of Nafion (referred to as an oligomer hereafter, shown in Figure 2(a)) was built. It is made up of a side chain -O-CF_2-C(F)(CF_3)-O-CF_2CF_2-SO_3^- and a fluorocarbon backbone to

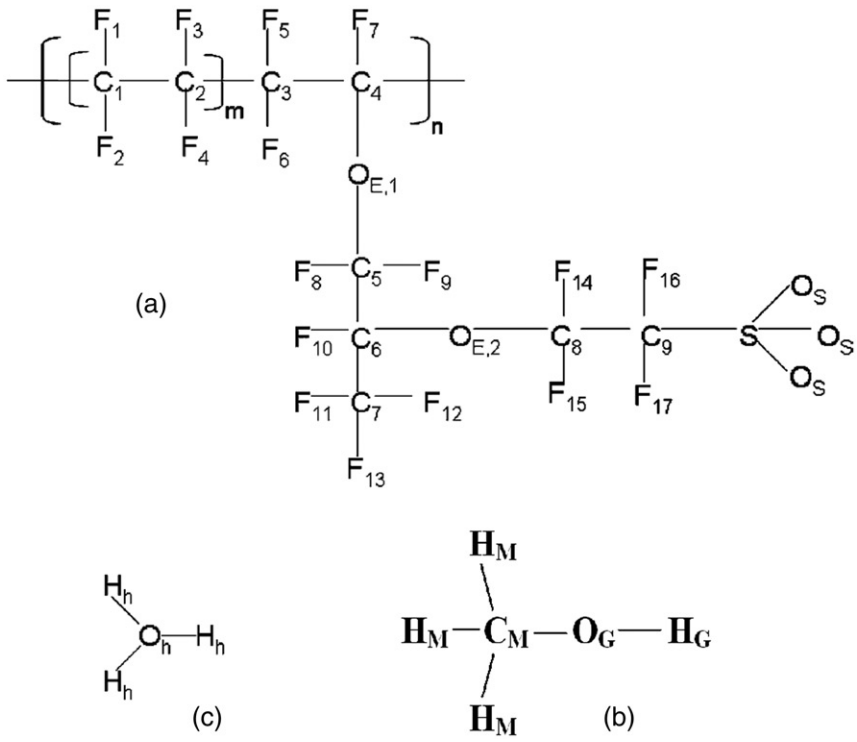

Figure 2. Chemical structure of (a) ionized Nafion, (b) methanol molecule, and (c) hydronium ion.

which the side chain is attached. To produce a Nafion single chain, 9 oligomers are attached to each other, consecutively. This task was done by using Gaussview software [44].

The Nafion's single chain is surrounded by a rectangular periodic box of TIP3P water molecules [45] that extended to at least 10 Å from the boundary atoms of Nafion (see Figure 5 of Ref. 43) using visual molecular dynamics (VMD) graphics program [46]. Creating such a rectangular periodic water box leads to the minimum distance of at least 20 Å between Nafion structure and another one situated in the vicinity box. By using the VMD autoionize plugin, to neutralize the system, sodium ions were added randomly to the simulation box. The number of added sodium ions is equal to the number of sulfonate groups. There are no adding negative charged ions. The resulting structure was then minimized through 10,000 steps. This was followed by a simulated annealing procedure using an *NVT* ensemble that involved four steps: (a) the final structure is obtained from the minimization step which was heated from 300 to 600 K over a period of 50 ps; (b) the final configuration obtained in step (a) was used as input for a subsequent MD simulation performed at 600 K for a period of 100 ps; (c) the final configuration obtained in step (b) was taken as the initial configuration for a MD simulation with cooling from 600 to 300 K over a period of 50 ps; finally (d) a MD simulation was performed at 300 K for 100 ps. The single chain of Nafion was then extracted and considered as a template for building the model systems. The chain was replicated using one of its symmetry planes to produce two chains across each other. The last structure was then replicated in one direction to produce five double chains (see Figure 6 of Ref. 43). The TIP3P water molecules that are extended to at least 10 Å from the Nafion atoms were added. To neutralize the system, an appropriate number of sodium ions (equal to number of sulfonate groups) were added. The above mentioned minimization and annealing procedures were repeated. In order to do the final step for producing the model, the ending structure of Nafion was extracted. An appropriate number of hydronium ions (equal to number of sulfonate groups), TIP3P water molecules, and methanol molecules are added. The extent of membrane hydration is typically denoted by λ, which shows the number of water molecules per sulfonic acid group. To determine the number of solvent molecules of each system, we first calculate the number of solvent molecules for a system with 15 water molecules per sulfonic acid ($\lambda = 15$) in the absence of methanol (weight percentage of methanol in membrane is zero). The total number of solvent molecules for other systems is set to be the same as that

Table 1. Description of six systems. The weight percentage of Nafion, methanol molar fraction, numbers of water and methanol molecules as well as hydronium ions added to each system are given. The density of each system at the end of simulation is given.

System	Methanol molar fraction	Methanol solution, wt%*	No. H_3O^+	No. H_2O	No. CH_3OH	Density ($g\,cm^{-3}$)
1	0	0	90	1260	0	1.70
2	0.03	5	90	1221	39	1.61
3	0.06	10	90	1181	79	1.64
4	0.13	20	90	1094	166	1.64
5	0.29	40	90	892	368	1.62
6	0.49	60	90	644	616	1.58

*wt% Methanol $= \frac{\text{Total weight of } CH_3OH}{\text{Total weight of } CH_3OH+H_2O+H_3O^+} \times 100$.

of the mentioned system. We then calculated the number of water and methanol molecules with regard to the above constraint to carry out MD simulation of Nafion swollen in the solutions with 5, 10, 20, 40, and 60% (weight percentage) of methanol. The simulated conditions for different systems are summarized in Table 1. The initial size of the simulation box for all systems is $43\,Å \times 46\,Å \times 193\,Å$.

We aim to carry out simulations for systems with a density close to experimental value. Experimental density of the neutral form of Nafion (15 water molecules per each sulfonic acid group) at 300 K is reported to be $1.75\,g/cm^3$ [47,48]; therefore, a minimization step was done and the annealing procedures now in *NPT* ensemble were repeated three times. This step was followed by a 4 ns MD simulation using the *NPT* ensemble. In all procedures, the 'wrapall' command was assigned to *on*. If a molecule crosses the periodic boundary, leaving the cell, setting this command to *on* will translate its coordinates to the mirror image of the opposite side of the cell. The trajectories obtained from the last 2 ns *NPT* ensemble were used to compute the structural properties. In order to find dynamic properties of water and methanol molecules as well as hydronium ions, the simulation has been continued for 2 ns, using the *NPT* ensemble, but now 'wrapall' command was assigned to *off*.

2.2. *Simulation parameters*

All simulations are performed using NAMD package [49], Langevin dynamic with a damping coefficient of $0.5\,ps^{-1}$, and Nose-Hoover Langevin piston [50] with a piston period of 200 fs and a decay time of 100 fs for keeping temperature (300 K) and pressure (1 atm) constant, respectively. The AMBER 99/GAFF force field [51,52] is used to compute the forces among Nafion atoms. This force-field has already been used in other MD simulations of Nafion [43,53]. Partial charges for the Nafion membrane are computed elsewhere [39]. The force field and partial charges for methanol molecules are taken from Charmm General Force Field/topology [54]. The force field parameters and partial charges for hydronium ions are taken from the Kusaka model [55]. The partial charges for the polymer, water and methanol molecules, and hydronium ion atoms are listed in Table 2. However, it should be noted that all the formal charges presented in Table 2. especially for hydronium ions could be different from the real charges [56]. Such differences could occur based on simulation condition and particularly because of charge transfer. Since partial charges have a very significant effect on molecular interactions, it is expected to get results with some variations from experimental values. Such variations could be seen at different degrees of short range (local) structure as well as solvent dynamics. The particle mesh Ewald (PME) algorithm [57] was used to calculate the long-range electrostatic interactions. The van der Waals forces are treated using a cutoff of 12 Å. Equations of motion were integrated with a time step of 1 fs.

3. Result and discussion

3.1. *Membrane morphology*

3.1.1. *Solvent clusters*

A final snapshot of MD simulation for different systems shows that the position of one sulfonate group relative to two across sulfonate groups is similar, shown in Figure 3. Movement of the neighbouring Nafion's single chains will result in a specific pattern for sulfonate distribution. Solvents are able to move in direction of the X-axis (see Figure 5 of Ref. 37 for definition of axes) freely, but the unity of solvents is completely broken in the direction of the Y-axis by

Table 2. Partial charges of ionized Nafion, methanol, and hydronium atoms. See Figure 2 for explanation of the labels on atoms.

Atom	Partial atomic charge	Atom	Partial atomic charge[a]
S	1.4124	F10	−0.1913
O_S	−0.632	C5	0.3228
C9	0.3216	F8, F9	−0.1637
F16, F17	−0.3278	C4	0.3218
C8	0.3218	F7	−0.1641
F14, F15	−0.1662	$O_{E,\ 1}$	−0.2742
$O_{E,\ 2}$	−0.2604	C(skel)*	0.3846
C7	0.4947	F(skel)**	−0.1923
F11, F12, F13	−0.1649	O_h	−0.248
C6	0.4010	H_h	0.4160
C_M	−0.0400	O_G	−0.6500
H_M	0.0900	H_G	0.4200

*Carbon atoms of fluorocarbon backbone except for C4.
**Fluorine atoms of fluorocarbon backbone expect for F7.
[a]Total charge of each Nafion's side chain is −1.

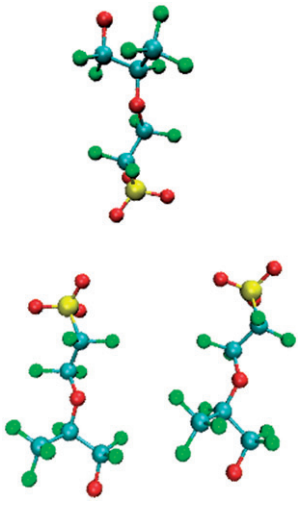

Figure 3. Relative positions of three sulfonate groups: one from a layer and the others from cross layer. Atoms are coloured as follows; S (yellow), O (red), C (dark green), and H (light green).

hydrophobic backbones, and strongly restricted in the direction of the Z-axis by sulfonic acid clusters of the up and down layers. As Table 1 shows, the density of the system reduces with increasing methanol concentration, which means that the membrane is swelled by uptake of methanol molecules in the MD simulation. This trend was produced in MD simulations reported by others [28,29]. Lee *et al*. utilized a novel combination of small and wide-angle neutron scattering methods to study local and long-range structure of

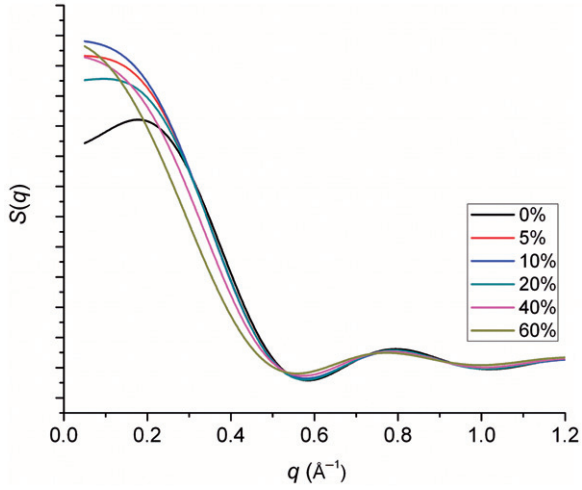

Figure 4. The structural factors estimated as the Fourier transform of the radial distribution functions for solvent oxygen.

water in Nafion 117 membranes [58]. To estimate the size of the solvent cluster (diameter of local solvent pools in the membrane), the structural factor '$S(q)$' of solvent oxygen atoms is calculated as the Fourier transform of the partial radial distribution function [RDF; $g(r)$] for oxygen atoms in both water and methanol as follows (for details on the formula, the method of obtaining solvent cluster size, and relationship between the solvent cluster size and ionomers cluster see Refs. 16, 58, 59, 60, and 61):

$$S(q) = 4\pi \frac{N}{V} \int [g(r) - 1] \frac{\sin(qr)}{q} r \, dr$$

Figure 4 presents the structural factor profile for each system. For the 0% solution, an apparent peak around $q = 0.18\ \text{Å}^{-1}$ ($r = 2\pi/q \sim 35\ \text{Å}$), which represents the solvent cluster, is observed. It should be noted that when the water content of Nafion is high, the structure of water in the clusters is predominantly that of bulk water. However, this situation may change at lower water contents where the water structure is likely to be more strongly influenced by water–sulfonic acid group interactions [16,58]. The peak obtained here matches to the typical diffraction peak observed experimentally by SANS and SAXS for perfluorinated ionomers [11,12,15,62–69]. Except for the solution with 20% methanol, for which there is a peak around $q = 0.10\ \text{Å}^{-1}$ ($r = 2\pi/q \sim 63\ \text{Å}$), there is no steadfast peak to be considered for calculation of the solvent cluster. The distribution is broaden with increasing methanol concentration. It is known that a higher concentration of methanol makes the boundary

between the aggregations of polymer matrixes and solvents ambiguous. In fact, based on the curves trends, our results show that considering a water–methanol mixture, the solvent cluster size in Nafion through the sandwich model increases when methanol concentration is enhanced. The electron spin resonance (ESR) and electron nuclear double resonance (ENDOR) measurements predict the size of the solvent cluster in the membrane swelled in methanol and methanol solution should be less than 20 Å [69,70]. It is worth noting that the mentioned observed cluster size is smaller than the experimental value for water-uptake membranes, which does not support our results. Our simulation results are not in agreement with the experimental observations even with regard to the proposal that the cluster should shrink with the addition of methanol. Therefore, the sandwich model, including our simplified approximations, is not able to predict experimental results for the relationship between cluster size and methanol concentration.

3.1.2. *Solvent coordination*

The radial distribution functions (RDF) for different selected atoms of different Nafion systems were calculated to quantify interactions among the sulfonate groups, water, methanol molecules, and hydronium ions. Since the amount of water and methanol in different systems are different, for any RDF in which water and/or methanol molecules are involved, only the peak width and position will be used for the structural analysis, but height of the peaks cannot provide any additional information.

The RDF of sulfur–sulfur for different systems is shown in Figure 5(a). Since the number of sulfur atoms in all systems is the same, we can consider the peak heights to gain more structural information. The height of the main peak for the 0, 5, 10, 20, and 40% solutions is roughly the same, but for the 60% solution it is reduced. The position of the main peak for the 5, 10, 20, 40, and 60% solutions is roughly the same, with a shift to the left relative to the 0% solution. This result shows that sulfonic acid groups are able to come closer to each other when there is some methanol present. The result also shows that above 5% solution, the methanol concentration is not responsible for the closeness of sulfonic acid groups. On the other hand, a second peak appears when methanol is present (Figure 5(a)). Note that the height of the second peak is very noticeably increased going from the 0 to the 5% solution, but increases only gradually for subsequent increased solutions. The results show that increasing methanol concentration may result in the formation of sulfonic acid clusters (Figure 5(a)). This means that the subsequent layers are formed by increasing methanol concentration. For the 5, 10, 20 and 40% solutions, formation of the second layer is due to decreasing disordered sulfur atoms beyond the second peak. But for the 60% solution, formation of the second layer is due to decrease of the first peak, which means that the number of sulfur atoms in the first shell reduces.

For all systems, the hydronium ions serve as bridges between the sulfonate groups. The RDF of sulfur atom and oxygen atom of hydronium ions for the different solutions is presented in Figure 5(b). The first peak of the RDF for all systems appears around 3.90 Å as reported by others [43,53], but farther than that reported for $g_{S\text{-}Li}(r)$ [29]. Such an increase in distance is logical owing to the larger size of the hydronium ion as well as its components. However, characteristic of all the systems studied here and Ref. 29, is the high degree of short-range (local) structure that is evident in the Li^+–S, and H_3O^+–S correlation functions. Such a feature is linked to the formation of ionic bonds between the sulfonate groups and Li^+, as well as H_3O^+. The number of neighbouring hydronium ions around a sulfur atom is computed directly using VMD software which provides accurate coordination numbers (Table 3). The cutoff of integration is 4.60 Å. This approximated cutoff corresponds to the first minimum of the RDF. As Table 3 shows, increasing methanol concentration does not change the number of neighbouring hydronium ions around a sulfur atom and such a coordination number is independent of methanol concentration. This result is not in agreement with that observed with Li^+ instead of hydronium as counterion. Chertovich *et al*. have shown that Li^+ ions get closer to the sulfonate acid groups in the presence of methanol, compared with pure water [29]. Our result indicates that although increasing methanol concentration will result in closer sulfonic acids to each other to some extent, when sulfonate groups are too close to each other, insertion of new hydronium ions is not easy because of the vdW repulsions. On the other hand, it is interesting to note that the second peak in Figure 5(b) is shifted to the right and narrower with increasing methanol concentration. Such an increase in the second peak was also reported for a system containing Li^+ instead of H_3O^+, which was interpreted as being due to the formation of a stronger second coordination shell [29]. Our result is predictable on the basis of sulfur–sulfur RDF. Such anRDF shows that increasing methanol concentration leads to formation of the second layer of sulfonic acid groups in better therefore, since hydronium ions serve as bridges between sulfonate groups, formation of second layer of hydronium ions around sulfonic acid groups should be better

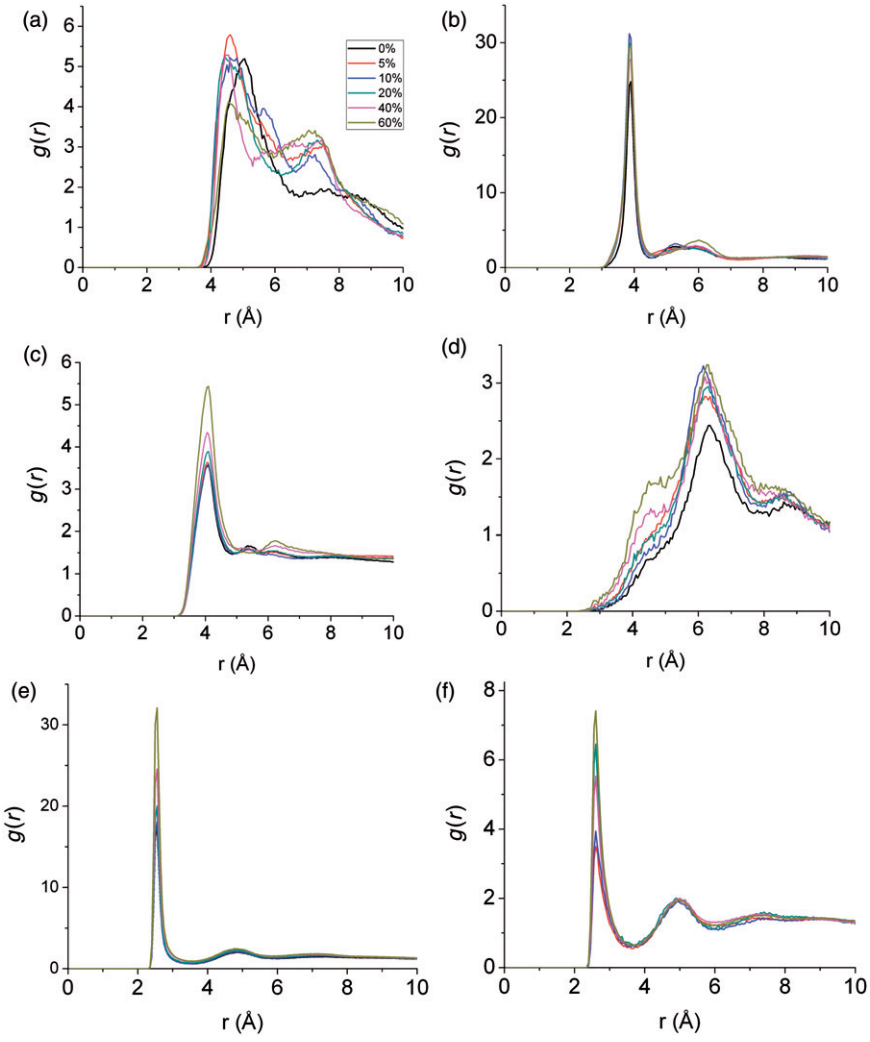

Figure 5. Radial distribution function for (a) S–S, (b) S–O_h, (c) S–O_t, (d) O_h–O_h, (e) O_h–O_t, and (f) O_h–O_G for the five systems, obtained from simulations. O_t is the oxygen atom of water molecule. For the other subscripts, see Figure 2.

ordered as well. The RDF of sulfur–sulfur shows that by enhancement of methanol content, the first peak is made wider; therefore, the main peak of the hydronium–sulfur RDF is expected to be wider, as is the case.

The water oxygen atom and sulfur atom RDF for different systems are presented in Figure 5(c). This figure shows that augmentation of methanol concentration affects the first shell of water molecules around sulfonic acid groups, making it broader. Such an affect makes sense based on the sulfur–sulfur RDF, as for the hydronium ion shell around sulfonic acid groups (see above discussion). It is worth noting the right shift of the second peak. This shift is due to the insertion of methanol molecules instead of water molecules around sulfonic acid groups. More methanol molecules will result in more insertions around sulfonic acid groups, which means pushing the second layer of water molecules further from the sulfonic acid groups. The number of water molecules around a sulfur atom presented in Table 3 shows a decreasing trend with increasing methanol concentration. This behaviour should be discussed from the following viewpoints: (a) decreasing water molecules in the whole system; (b) interaction energy of sulfonic acid groups with water and methanol molecules; (c) molecular size and electrostatic properties; and (d) interactions with other parts of Nafion. Intermolecular interaction energies of water and methanol molecules with sulfonic acid group are almost the same. Values of the interaction energies are -10.52 and -10.38 kcal/mol for the most stable configuration of $CF_3OCF_2CF_2SO_3^- + H_2O$ and $CF_3OCF_2CF_2SO_3^- + CH_3OH$ at the MP2/aug-cc-pVDZ//B3LYP/6-31+G* level [71–77] of molecular orbital

Table 3. The calculated number of neighbouring molecules obtained via the RDFs. Note that the left atom is the central and the right one is the surrounding species of the central atom. For all computations, the number of neighbouring molecules is obtained by integrating the area under the main peak of the corresponding RDF.

(a)

Methanol solution, wt%	S–H_2O	S–H_3O^+	S–$HOCH_3$	H_3O^+–H_2O	H_3O^+–$HOCH_3$[a]	$HOCH_3$–CH_3OH[b]
0	7.22	1.55	–	3.83	–	–
5	6.78	1.53	0.13	3.65	0.08	0.38
10	6.80	1.55	0.18	3.49	0.12	0.69
20	6.67	1.53	0.39	3.60	0.22	1.63
40	6.14	1.47	1.04	3.52	0.65	3.45
60	5.47	1.51	1.59	2.97	1.23	5.65

(b)

	CH_3OH–$HOCH_3$[c]	H_2O–H_2O	CH_3OH–H_2O[d]	Backbone–CH_3OH[e]	Backbone–H_2O
0	–	3.92	–	–	0.82
5	0.07	3.88	2.86	0.15	0.65
10	0.11	3.81	3.07	0.31	0.61
20	0.27	3.60	2.86	0.63	0.41
40	0.61	3.11	2.32	1.17	0.23
60	1.00	2.28	1.66	1.51	0.12

[a]Number of neighbouring methanol molecule around hydronium ion via the methanol OH head.
[b]Number of neighbouring methanol molecule around a given methanol via CH_3 head.
[c]Number of neighbouring methanol molecule around a given methanol via OH head
[d]Number of neighbouring water molecule around a given methanol via OH head.
[e]Number of neighbouring methanol molecule around the hydrophobic backbone via CH_3 head.

calculations [41,76]. Therefore, it is reasonable to see a decreasing trend in the number of water molecules around sulfonic acid groups due to water content reduction. On the other hand, the number of methanol molecules has an increasing trend as expected, but it is interesting to note that for all systems, the number of neighbouring water molecules is more than the number of methanol molecules. Such an observation is even true for the 60% solution in which the total number of water and methanol molecules is roughly the same. In such a system, the number of water molecules surrounding a sulfonic acid group is approximately 3.4 times more than the number of methanol molecules. To justify the above behaviour, the factor of molecular size along with its interactions with other parts of Nafion should also be taken into account. The water molecule is smaller and more polar than methanol, which allows the continuous formation of water clusters, but the methanol molecule is bigger and has polar and also nonpolar parts. Having a bigger size does not favour aggregation as much as smaller molecules in a constant volume. On the other hand, although association of methanol molecules with sulfonic acids is more energetically favourable than with the other sites in the chain, such as CF_3 and ether oxygen [41,76], having a hydrophobic part (methyl) gives a stronger force to be further from the sulfonic acid group (a hydrophilic group) and approach the hydrophobic backbone of Nafion. Table 3 indicates that methanol molecules prefer to aggregate around sulfonic acid groups rather than self-aggregation via hydrogen bonding (polar aggregation). However, methanol molecules prefer self-aggregation via the hydrophobic part (methyl) rather than association with the sulfonic groups and self-aggregation via hydrogen bonding. This table also shows that polar aggregation of methanol with water molecules is more probable than the polar self-aggregation as it was reported for the bulk solution of water-methanol mixture [77–79]. Such a conclusion may indicate that more control is needed for water managing during sending out of water from membrane in fuel cell condition work. Results for the number of neighbouring methanol molecules near the hydrophobic backbone of Nafion show that hydrophobic self-aggregation of methanol is more probable than gathering near Nafion's hydrophobic backbone. Table 3 shows that like methanol, water molecules prefer to interact with other water molecules; however, comparison of the two interactions shows that this preference in water molecules is much stronger than that of methanol molecules. For instance, in the 60% solution, the ratio of hydrophobic

self-aggregation of methanol molecule gathering near the hydrophobic backbone is 3.74 (5.65/1.51), while in the case of water it is 19 (2.28/0.12). Our results are in good agreement with those given by Saito *et al.* [80]. Their results show that the methanol permeability increased with decrease in the equivalent weight (EW) of some membranes. They suggested that methanol molecules penetrate into the hydrophilic regions to form ionic cluster regions together with water molecules and sulfonic acid groups, in a similar way to the membranes in the fully hydrated state, and diffuse through the expanded spaces [80]. However, comparing our results with theirs shows that formation of ionic cluster regions of methanol with water molecules is more significant than formation of such ionic clusters of methanol with sulfonic acid groups. On the other hand, hydrophobic self-aggregation of methanol molecules via CH_3 group is important, as well.

We have estimated number of water and methanol (considering either OH or CH_3 heads) molecules surrounding different specified pending group of a chain (Figure 6). It should be noted that solvent molecules (methanol and water) are highly populated in the vicinity of sulfonic acid groups, and the number of neighbouring solvent molecules decreases towards the main chain. There are some differences between water and methanol distributions along the pending group of a chain. In the case of water molecules, Figure 6(a) shows that increasing methanol concentration will result in a declining number of neighbouring water molecules around each part of the pending group. It is interesting to note that the slopes of such a figure from OE2 to S atoms are the same for all systems, which means methanol addition does not effect the increasing amount of neighbouring waters molecules around the pending atoms. However, this figure shows that methanol addition has a different effect on the increasing amount of neighbouring waters around OE1 to C19, which could be concluded from different slopes in the various systems. Figure 6(b) shows the number of methanol molecules from the OH head surrounding different atoms of the pending groups. This figure indicates that in comparison with water, methanol from OH head does have a much lower percentage of surrounding molecules around the pending groups. On the other hand, in contrast to the case of the slope of each part of the figure being different, it may be concluded that methanol addition has different effect on the increasing amount of neighbouring methanol from OH head for the pending atoms. Figure 6(c) shows number of methanol molecules from the CH_3 head, surrounding different atoms of the pending group. This figure indicates that at low levels of methanol concentration, methanol

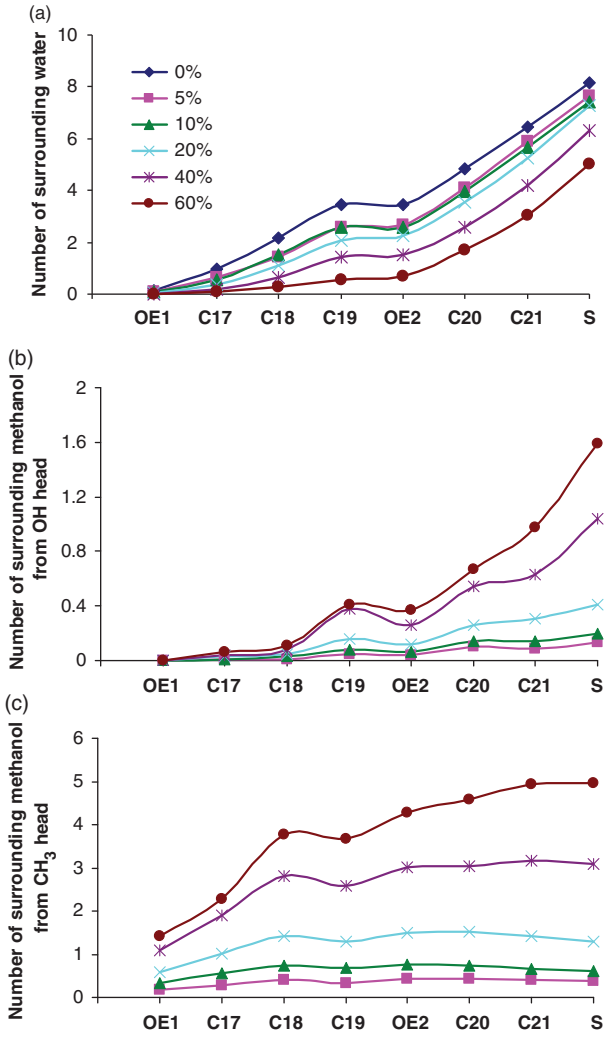

Figure 6. Number of (a) water and (b and c) methanol molecules surrounding each specified atom of the pending group of the chain. In the case of methanol molecules, two heads [(b) OH and (c) CH_3] are investigated. Cut-off for such calculations are 4.85 Å for water and 4.70 Å and 6.20 Å for methanol OH and CH_3 head, respectively. Such cut-offs correspond to first minimum of S–O (water), S–O (methanol) and C–C of methanol molecules in the RDFs.

(from CH_3 head) distribution is the same for each atom of the pending groups. However, increasing of methanol will lead to more uneven distribution.

Distribution of water and methanol molecules in nano-channels requires further analysis. We shall use the same classification for solvent molecules as used by others [34,43]. We classify solvent molecules into three categories: bonded solvent (**BS**), weakly bonded solvent (**WS**), and free solvent (**FS**). Solvent molecules which their oxygen atom lays within 4.85 Å from the sulfur atom of sulfonate group are considered to be **BS**. Those molecules whose S–O distance from a

sulfonate group is between 4.85 and 7.00 Å are considered as **WS,** and finally, **FS** molecules are those that the distance is larger than 7.00 Å. The results are summarized in Figure 7.

As Figure 7a shows, when the solvent is pure water, an approximately equal number of water molecules belongs to both **BS** and **FS** types. However, this figure indicates that the most water molecules should be classified as **WS**. On the other hand, a small amount of methanol molecules (in the 5% solution) will result in a distinguishable affect on the water distribution. Since as previously mentioned, methanol molecules are able to interact with sulfonic acid groups efficiently; therefore, to do so, a number of water molecules adjacent to sulfonic groups (**BS** and **WS**) should leave their positions and enter to the **FS** region; Figure 7(a) supports this idea. There will be enough space for

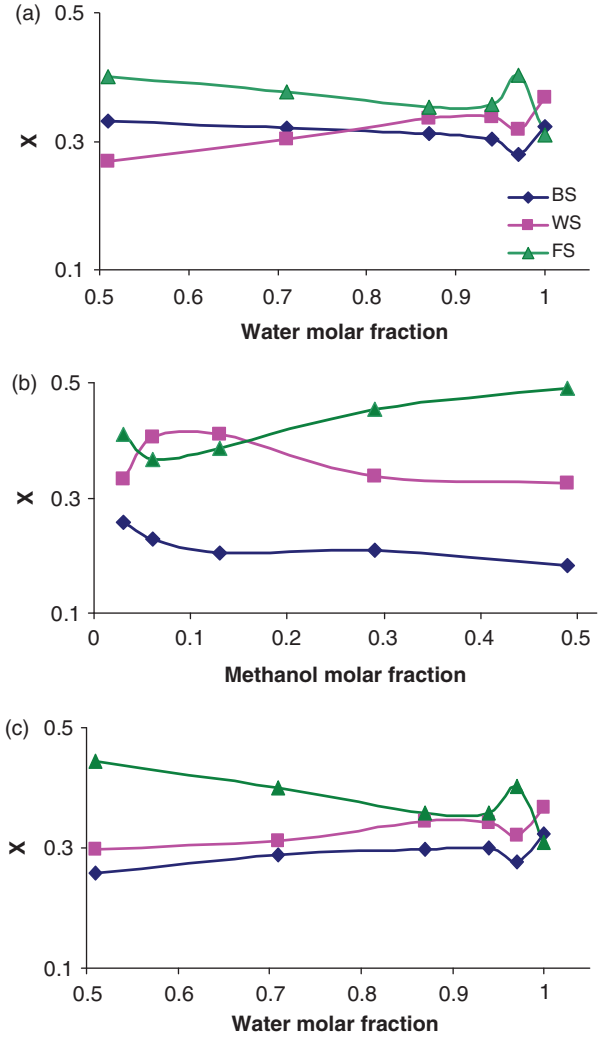

Figure 7. Fraction of (a) water, (b) methanol, and (c) water + methanol molecules (X) as the **BS**, **WS**, and **FS** types.

methanol molecules to approach sulfonic acid groups. This figure indicates that such solvent replacement up to 20% solution will lead to water molecules being mostly of **FS** category, then **WS** category, with the least in category **BS**. However, at the levels of 40 and 60% solutions, the positions of **WS** and **BS** are switched, which means **BS** is more probable than **WS**. This behaviour can be discussed based on the dielectric effect of the solvent. Since methanol dielectric is less than that of water, more methanol molecules in the system result in a system with less dielectric constant. In a system with less dielectric constant, ions and polar molecules will be closer to each other, therefore, since water molecules are much more polar than methanol molecules, they will stay closer to sulfonic acid groups.

Distribution of methanol molecules is presented in Figure 7(b). As this figure shows, at any level of methanol concentration, the **BS** type has the least weight, which is in accordance with the results given in the previous section on hydrophobic self- and with-water-aggregation, compared with gathering near sulfonic acid groups (Table 3). In the cases of **WS** and **FS**, two replacements in relative positions are observed as a function of methanol concentration. In the 5% solution more water molecules are free than those which are weekly bonded. However, in the 10 and 20% solutions, the relative fraction is reversed and more water is now belong to **WS** compared with **FS**, but it should be noted that the difference is not much. Then, in the 40 and 60% solutions **FS** type is again dominating relative to **WS**, but now, the difference becomes more and more with increasing methanol concentration. According to Table 3, up to the 20% solution, methanol molecules prefer to interact with water molecules more than like molecules (methanol) via the hydrophobic or hydrophilic self aggregation. Based on Figure 7(a)**,** the water molar fraction of the **WS** and **FS** in the 10 and 20% solutions is roughly the same and more than that of **BS**; therefore, it is expected to find methanol molecule in **WS** and **FS** region with the same probability. In the 40 and 60% solutions, Table 3 shows that the groups are formed via the hydrophobic parts (methyl) which needs to have enough space without disturbing the polar parts of Nafion (sulfonic acid groups). On the other hand, the **WS** for water has decreased significantly and reversely, the **FS** has increased in the 40 and 60% solutions. Such a phenomenon is due to the fact that methanol molecules which are interacting with water molecules have a tendency to go in the **FS** region of methanol. Therefore, the **FS** and **WS** of methanol are more different for these methanol concentrations. It is interesting to note that the differences in **BS**, **WS**,

and **FS** for the methanol molecules are more than those of water molecules. Such a difference may indicate that methanol distributes specifically more than water in the nano-channels of sandwich model.

Distribution of both solvent molecules (methanol + water) is shown in Figure 7(c). This figure clearly shows that a bit amount of methanol (the 5% solution) has an important impact on the total solvent distribution; **FS** increases and at the same time both **BS** and **WS** decrease. Such a result may be explained based on methanol characteristics. Large methanol molecules cannot get as close as water molecules to sulfonic acid groups. For the 10% solution, compared to the 5% solution, **FS** decreases and both **BS** and **WS** increase. This behaviour has already been seen for the water, which means the predominant effect of water distribution in whole solvent distribution. There is no difference for different types of water in the 20% and 10% solutions. This is expected since no significant change for any solvent distribution occurs in the mentioned concentration range. Behind the 20% solution, **FS** increases and **WS** decreases both with a significant rate. Also, the BS decreases but more slowly. One may note that such a behaviour has already been observed for methanol, which means the methanol distribution is predominant the whole solvent distribution in the system in such methanol concentration range.

To survey the structural relationship of hydronium ion with, water and methanol molecules as well as other hydronium ions, the RDFs of their oxygen are calculated and presented in Figure 5. As Figure 5(d) (hydronium ion oxygen-hydronium ion oxygen RDF) shows, more hydronium ions are able to approach the central hydronium ion which is due to decreasing solvent dielectric constant and hence approaching of sulfonic acid groups to each other, as previously discussed. It is interesting to note that the main peak is around 6.30 Å. It is a long distance due to surroundings sulfonic acid groups by hydronium ions. The proton transport mechanism in water may be viewed as a two steps mechanism: the jumping of protons between water molecules, called the Grotthuss mechanism [81], and the diffusion of the entire water complexes through the hydrogen bond network made by water clusters. The RDF of the oxygen atom of hydronium ion and the oxygen atom of the water molecules for different systems are shown in Figure 5(e). The first peak of the RDF for all systems appears around 2.55 Å, while the second wider peak around 4.85 Å, as previously reported for a non-sandwich model [53] and sandwich model in previous work [43]. It is worthwhile to note that substitution of hydronium ions by lithium ions will result in closing of positive counter ions (Li^+) to water solvent. It was shown that position of the first maxima in the RDF of Li–O for the water-containing system under *NPT* and *NVT* conditions is 2.1 Å, which is smaller than our result [29]. It should be noted that at high methanol concentrations, there are less water molecules around hydronium ions (Table 3). The hydronium ions oxygen-methanol oxygen RDF is shown in Figure 5(f) for different systems. There are two peaks for this RDF; the main peak appears around 2.60 Å and the second are around 5.00 Å. It is shown that as for water molecules, here for methanol molecules, the nature of interactions and shell formation around hydronium ions are not affected by the methanol concentration. It is obvious that more methanol molecules in whole system will result in more methanol molecules surrounding hydronium ions and then less water molecules surrounding hydronium ions. However; based on Table 3, for all systems, water molecules are the most dominating component surrounds sulfonic acid groups. Such domination is even true for the 60% solution (the ratio of surroundings water molecules to surrounding methanol molecules in this system is 2.41).

It is interesting to compare our results (data was not shown) on methanol oxygen-methanol oxygen RDF with those reported by Morrone *et al.* for methanol-water solutions using an ab initio molecular dynamics simulation [82]. Our results show that, hydrophilic self-aggregation of methanol in Nafion via OH group is ordered even at low methanol concentrations. There are two peaks in the mentioned RDF; the main peak appears around 2.95 Å and the second one is around 4.80 Å. However, results reported in Ref. 82. Indicats that oxygen–oxygen methanol structure is strongly depends on methanol concentration, in such a way that at high concentration such structure is improved while at low concentration is going to be ambiguous.

3.2. *Solvent dynamics*

Although the critical proton jumping mechanism is missing in our MD model, it is nevertheless interesting to investigate the water, methanol, and hydronium diffusions in the solutions. Their values can be estimated from the mean-square-displacement (MSD) for different species. The diffusion coefficient, D, was evaluated from the mean square displacement as follows:

$$D = \frac{\langle |r(t) - r(0)|^2 \rangle}{6t}$$

where $r(t)$ and $r(0)$ are the position of molecule at time (t) and zero, respectively. The calculated diffusion coefficient of water strongly depends on the model used for water molecules [83,84]. Since our goal is only to compare the diffusion coefficient of water molecules for different systems with different methanol concentration; therefore, using TIP3P model for water molecule does not influence on our conclusion. We will also compare our results with the others obtained for the bulk TIP3P of water molecules. Figure 8(a) shows the mean square displacement (MSD) of water molecules in various systems at 300 K. Table 4 presents the diffusion coefficient for H_2O in different simulated systems over the sampling period. It is interesting to note that the 5% solution shows a very slight MSD increscent relative to that of 0%. As previously discussed, a slight amount of methanol molecules (the 5% solution) will lead to increasing of **FS** and decreasing both **BS** and **WS**. Therefore, water MSD is anticipated to have a higher value as our result supports. On the other hand, Figure 8(a) shows that, there is no change for **FS**, **WS**, and **BS** of the 20% solution relative to the 10% solution which means that there is no difference between the MSD of these systems, as our results support it. However, Figure 8(a) points out that the MSD of water molecules has a degrading trend by increasing methanol content, behind the 20% solution. As Figure 7(a) shows, molar faction of water **BS** is increased gradually by addition of methanol, which means that relatively more water molecules are attached to sulfonic acid groups that make them unable to move because of the strong electrostatic interactions. On the other hand, molar fraction of water **FS** is increasing by addition of methanol as well; therefore, to get a reasonable understanding, the increment should be taken into account as well. It will be helpful if this category (**FS**) is considered as a pure mixture of water–methanol. Previous studies on water–methanol mixtures have shown that diffusion of water molecules is decreased through enhancement of system by methanol molecules up to approximately 0.5 molar fraction of methanol. There have been noticeable investigations on the microstructure of methanol and its aqueous solutions via both experiment and theory; this is motivated by the observation of greater deviations of dynamic and excess thermodynamic properties from ideal mixing behaviour at low to mid-ranges of methanol concentration [83–86]. This anomalous behavior is linked to the formation of some unique microstructure (enhanced water structure around alcohol methyl groups; molecular-scale immiscibility leading to a microemulsion environment, particularly at high alcohol concentrations).

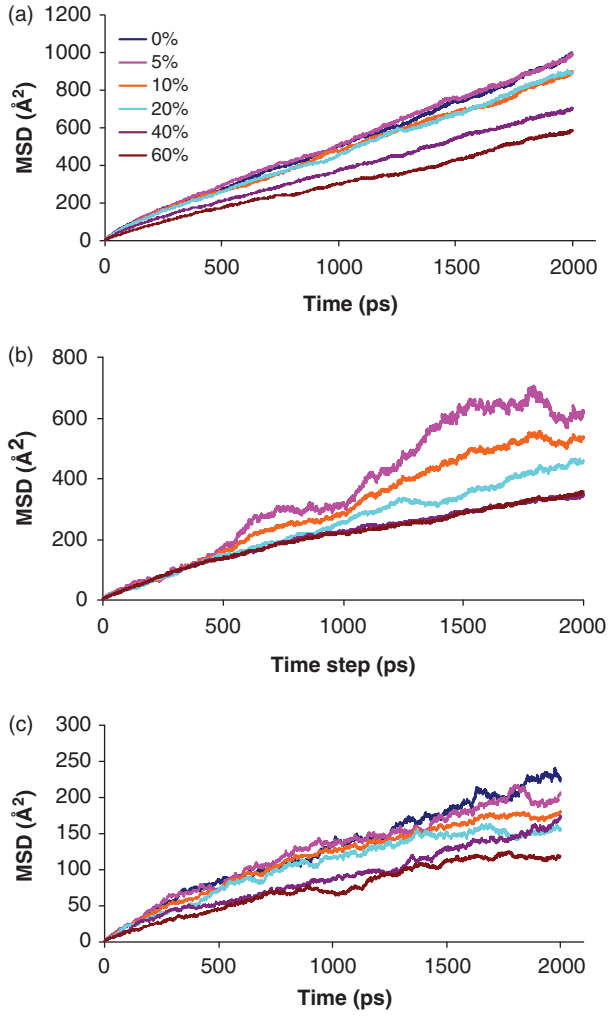

Figure 8. Mean-square-displacement of (a) water, (b) methanol, and (c) hydronium as a function of simulation time.

Extensive neutron diffraction experiments coupled with atomistic simulations of aqueous methanol solutions have recently shed a light on the bipercolating network structure of methanol–water solutions over extended concentration ranges [77]. Our results which indicates decreasing trend of water diffusion is in accordance with the previous results of others [79,85–88]. However, such a result is not in agreement with the system containing Li^+ instead of H_3O^+ ions. In the mentioned system, the value of D_{H_2O} initially increases with methanol concentration (c_m) increasing up to $c_m \approx 0.5$ and then decreases [29]. The molecular dynamics simulation of TIP3P water molecules by others shows that diffusion coefficient for the mentioned model is $5.60 \times 10^{-5}\,cm^2/s$ at 300 K [89,90]. These results indicate that diffusion of water molecules in the polymer is less than that of water in the pure bulk state which is experimentally supported for

Table 4. Diffusion coefficients of water and methanol molecules along with hydronium ions for the six solutions at 300 K. The ratios of calculated diffusion coefficient for bulk TIP3P water molecules to that calculated for water molecules in Nafion ($D_{TIP3P}/D_{wat\text{-}Naf}$), diffusion coefficient for water molecule in Nafion to that for hydronium ion in Nafion ($D_{wat\text{-}Naf}/D_{hyd\text{-}Naf}$), diffusion coefficient for water molecule in Nafion to that for methanol in Nafion ($D_{wat\text{-}Naf}/D_{met\text{-}Naf}$), and diffusion coefficient for methanol molecule in Nafion to that for hydronium ions in Nafion ($D_{met\text{-}Naf}/D_{hyd\text{-}Naf}$).

Methanol solution, wt%	D (H_2O) ($\times 10^{-5}$ cm^2/s)	D (CH_3OH) ($\times 10^{-5}$ cm^2/s)	D (H_3O^+) ($\times 10^{-5}$ cm^2/s)	$D_{TIP3P}/D_{wat\text{-}Naf}$	$D_{wat\text{-}Naf}/D_{hyd\text{-}Naf}$	$D_{wat\text{-}Naf}/D_{met\text{-}Naf}$	$D_{met\text{-}Naf}/D_{hyd\text{-}Naf}$
0	0.82	–	0.18	6.81	4.55	–	–
5	0.83	0.51	0.17	6.76	4.88	1.63	3.00
10	0.74	0.44	0.15	7.55	4.93	1.68	2.93
20	0.74	0.38	0.13	7.55	5.69	1.95	2.92
40	0.59	0.29	0.14	9.53	4.21	2.03	2.07
60	0.49	0.30	0.10	11.50	4.90	1.63	3.00

Nafion [87–91]. Our survey shows that diffusion coefficient of bulk water is greater, approximately by 6.8 to 11.5 times, which is in good agreement with those results obtained for the system containing Li^+ instead of H_3O^+ [29].

Figure 8(b) shows the mean square displacement (MSD) of methanol molecules for different solutions at 300 K. As this figure shows, the MSD of methanol is decreased via addition of methanol. On the contrary to water case, such a result is not in agreement with the system containing Li^+ instead of H_3O^+ [29]. It is worth mentioning that differences in MSD for low concentrations are remarkable but, the difference will be decreased after enhancement of solutions with methanol molecules. To give an explanation for such a behaviour, four types of interactions which effect on the methanol molecules movement should be taken into account; its interactions with (a) sulfonic acid group, (b) hydrophobic backbones, (c) water molecules, and (d) other methanol molecules especially via hydrophobic part (methyl). Figure 7(b) shows that the molar fraction of interacting methanol molecules with sulfonic acid groups is decreased very slightly by upgrading of methanol content; therefore, from this point of view the movement should be easier. On the other hand, the methanol molecules far from sulfonic acid groups are interacting with hydrophobic backbone, water molecules, or other methanol molecules which all of them reduce the methanol movement. After saturation of the hydrophobic backbone with methanol molecules, addition of such molecules should definitely go to pseudo-typical water–methanol mixture and interact with them. So our prediction would be decreasing methanol diffusion to some extent and then seeing typical behaviour of water–methanol mixture. Our results are completely in agreement with such a conclusion. Results show that, MSD of methanol molecules is firstly decreased and then will be constant to some extent (Figure 8(b)). The previous reported data by others shows that, methanol diffusion in the water-methanol mixture has no remarkable changes approximately within 0.2 to 0.4 methanol molar fraction [77,92]. Since we have presumed that some of methanol molecules are responsible for covering the hydrophobic backbone, molar fraction of methanol in our pseudo- water–methanol mixture between two hydrophobic backbones is less than the actual molar fraction. Therefore, as it is presented in Figure 8(b) and Table 4, self-diffusion of methanol molecules for the 40 and 60% solutions is roughly the same. Table 4 also shows that diffusion of water is more than methanol molecules (approximately by a factor of 1.6 to 2.0 times) in all concentrations which is supported by the previous theoretical and experimental data [77,92–94]. However, the related results for the system containing Li^+ instead of H_3O^+ have indicated that diffusion of water is less than methanol molecules. Such results were explained on the basis of system densities [29].

Figure 8(c) shows the mean square displacement (MSD) of hydronium ions for the different solutions at 300 K. The diffusion coefficient for the hydronium ions was determined to be much smaller than that for water (by a factor of 4.2–5.7) and methanol (by a factor of 2.1–3.0). Considering the strong electrostatic attractions among hydronium ions and the negatively charged sulfonate groups, such a low diffusion is expected. This figure indicates that at higher methanol concentrations, hydronium ions have smaller diffusion coefficient. This is completely reasonable due to decreasing of solution dielectric constant. With more methanol content, the dielectric constant of the system will be declined and then, the electrostatic interactions of ions will be more noticeable. In such circumstances,

the hydronium ions are attached to sulfonic acid groups more strongly which may result in decreasing of the diffusion coefficient. Such a result is also in good agreement with experimental data reported by Saito *et al*. [82]. Their results indicate that the proton conductivity is reduced by methanol penetration into the membranes especially for the smaller EW value ones. To investigate the roles of CH_3 group of methanol, they measured self-diffusion coefficients of the alkyl group D_{CH_3} and of OH (including protons) D_{OH} of different alcohols (methanol, ethanol and 2-propanol). Both coefficients values increased with decreasing the EW value, and the D_{OH} was always larger than the D_{CH_3}. In addition, the differences between the D_{OH} and D_{CH_3} increased with the decrease of the size of alkyl groups [82]. They interpreted that, that protons transport faster than the alcohols by the Grotthuss (hopping) mechanism, and the faster proton transport was promoted more when the membrane was penetrated by smaller alcohol. The diffusion of hydronium ions; here, could not be compared with the experimental value if the absolute value is of interest, because we have only computed the vehicular transport of H_3O^+, while the measured proton transport includes hopping of the bare H^+ among water molecules, as well. On the other hand, *ab initio* molecular dynamics simulation of methanol-water solutions reveals the existence of separate hydrogen-bonded water and methanol networks [82]. Such a study shows also that Grotthuss type of diffusion mechanism of the proton in which water-to-water, methanol-to-water, and water-to-methanol proton transfer reactions play the dominant role in proton diffusion while, methanol-to-methanol transfers being much less significant [82].

However, since Li^+ transport is vehicular, it is interesting to compare our results with those obtained by Chertovich *et al*. for the system containing Li^+ instead of H_3O^+ [29]. Their simulation values of D_{Li^+} was $0.7 \times 10^{-5}\,cm^2/s$, which is higher than those obtained here for hydronium ions [29]. Such a reduction in self diffusion could be related to the strong hydrogen bonds of hydronium ions and sulfonic acid groups, as well as solvent molecules.

4. Conclusion

The results presented in this work highlight the crucial role of methanol content on the hydrated Nafion structure and solvent transport properties. The method is based on the molecular dynamics simulation of the sandwich model which is a simplified model. Our initial structures are created in such a way that the distance between sulfonate groups of two neighboring layers is minimum. Studying the model with the maximum distance could be helpful for a deep understanding of the sandwich model. The other simplification is using the periodic boundary conditions to make the model continuous. Such a condition also allows the thickness parameter to be discarded. Taking the mentioned parameter into account can be an interesting topic for further investigations. Statistical structural factor evaluated as a Fourier transform of a partial RDF profile of solvent oxygen shows that the peak that represents the cluster size shifts toward a smaller value of q and becomes broader with increasing methanol concentration. This implies although boundary between the aggregations of polymer matrixes and solvents is going to be ambiguous, a more-spherical solvent cluster is formed in the membrane immersed in a solution with higher methanol concentration. We presume that this phenomenon is due to the nature of methanol as well as the simplified model which has been studied in this work. The calculated number of water and methanol molecules surrounding different specified groups within Nafion shows that methanol can more easily approach a hydrophobic polymer matrix, in comparison with water. On the other hand, water is situated nearer the sulfonic acid group, compared to methanol, even though both have similar attractive interaction energies with the acidic group. Analyzing of solvent distribution shows that presence of a slight amount of methanol molecules (even 5%) will result in a significant affect on the water distribution. Such analyzing shows that the methanol distribution is more specific than that of water in nanochannels, as well. Structural analysis shows that the sulfonic acid clusters in high methanol concentration is much ordered so that subsequent layers are able to be formed. It was also found that although the first shell of hydronium and water around the sulfonic acid clusters become broader by increasing methanol concentration, the number of neighboring hydronium ions around a sulfur atom is not affected by the concentration change. The diffusion coefficient of solvent was also analysed as a function of methanol concentration. It was shown that for the three components; water, methanol, and hydronium, the coefficient has a declining trend. It was discussed that many changes of solvent properties may be related to the dialectic constant of solution.

References

[1] K.D. Kreuer, S.J. Paddison, E. Spohr and M. Schuster, Chem. Rev. **104**, 4637 (2004).

[2] H.R. Allcock, N.J. Sunderland, R. Ravikiran and J.M. Nelson, Macromolecules **31**, 8026 (1998).
[3] F.M. Gray, *Solid Polymer Electrolytes, Fundamentals and Technological Applications* (Wiley-VCH, New York, 1991).
[4] V. Mehta and S.J. Cooper, J. Power Sources **114**, 32 (2003).
[5] O. Borodin and G.D. Smith, Macromolecules **31**, 8396 (1998).
[6] T.S. Zhao, K.D. Kreuer and T. Van Nguyen, *Advances in Fuel Cells* (Elsevier, Oxford, 2007).
[7] J. Ennari, Polymer **49**, 2373 (2008).
[8] K.D. Kreuer, Chem. Mater. **8**, 610 (1996).
[9] S. Gottesfeld, T.A. Zawodzinski, R.C. Alkire, H. Gerischer, D.M. Kolb and C.W. Tobias, *Advances in Electrochemical Science and Engineering* (Wiley-VCH, Weinheim, 1997).
[10] E.J. Roche, M. Pineri, R. Duplessix and A.M. Levelut, J. Polym. Sci. Polym. Phys. Ed. **19**, 1 (1981).
[11] T.D. Gierke, G.E. Munn and F.C. Wilson, J. Polym. Sci. Polym. Phys. Ed. **19**, 1687 (1982).
[12] J.A. Elliott, S. Hanna, A.M.S. Elliott and G.E. Cooley, Macromolecules **33**, 4161 (2000).
[13] G. Gebel and R.B. Moore, Macromolecules **33**, 4850 (2000).
[14] B. Loppinet, G. Gebel and C.E. Williams, J. Phys. Chem. B **101**, 1884 (1997).
[15] C. Gebel, Polymer **41**, 5829 (2000).
[16] K.A. Mauritz and R.B. Moore, Chem. Rev. **104**, 4535 (2004).
[17] W.Y. Hsu and T.D. Gierke, J. Membr. Sci. **13**, 307 (1983).
[18] H.L. Yeager and A.J. Steck, J. Electrochem. Soc. **128**, 1880 (1981).
[19] K.A. Mauritz, C.J. Hora and A. Hopfinger, in *J. In Ions in Polymers*, edited by A. Eisenberg (American Chemical Society, Washington DC, 1980).
[20] V.K. Datye, P.L. Taylor and A. Hopfinger, Macromolecules **17**, 1704 (1984).
[21] K.A. Mauritz and C.E. Rogers, Macromolecules **18**, 483 (1985).
[22] B. Dreyfus, Macromolecules **18**, 284 (1985).
[23] M. Eikerling, A.A. Kornyshev and U. Stimming, J. Phys. Chem. B **101**, 10807 (1997).
[24] H.G. Haubold, T. Vad, H. Jungbluth and P. Hiller, Electrochimica Acta **46**, 1559 (2001).
[25] H.Y. Ryu and J.B. Benziger, *A study of methanol vapor sorption dynamics by Nafion membranes* (BS thesis, Department of Chemical Engineering and Material Science Certificate Program, Princeton University, 2009).
[26] G.J. Elfring and H. Struchtrup, *Thermodynamics of sorption and distribution of water in Nafion* (MS thesis, Department of Mechanical Engineering, University of Victoria 2005).
[27] K.D. Kreuer, J. Membr. Sci. **185**, 29 (2001).
[28] R.S. Mclean, M. Doyle and B.B. Sauer, Macromolecules **33**, 6541 (2000).
[29] A. Chertovich, P.G. Khalatur and A.R. Khokhlov, Compos. Interf. **16**, 547 (2009).
[30] A. Kuver and W. Vielstich, J. Power Sources **74**, 211 (1998).
[31] M.K. Ravikmar and A.K. Shukla, J. Electrochem. Soc. **143**, 2601 (1996).
[32] A. Heinzel and V.M. Barragan, J. Power Sources **84**, 70 (1999).
[33] J. Cruickshank and K.J. Scott, Power Sources **70**, 40 (1998).
[34] S. Urata, J. Irisawa, A. Takada, W. Shinoda, S. Tsuzuki and M. Mikami, J. Phys. Chem. B **109**, 17274 (2005).
[35] D.N. Theodorou, Mol. Phys. **102**, 147 (2004).
[36] B. Kvamme, G. Huseby and O. Fmrrisdahl, Mol. Phys. **90**, 979 (1997).
[37] Y. Peng and C. Mccabe, Mol. Phys. **105**, 261 (2007).
[38] S.D. Miranda Tomasio and T.R. Walsh, Mol. Phys. **105**, 221 (2007).
[39] A. Vishnyakov and A.V. Neimark, J. Phys. Chem. B **105**, 7830 (2001).
[40] A. Vishnyakov and A.V. Neimark, J. Phys. Chem. B **104**, 4471 (2000).
[41] S. Urata, J. Irisawa, A. Takada, S. Tsuzuki, W. Shinoda and M. Mikami, J. Fluorine Chem. **126**, 1312 (2005).
[42] C.V. Mahajan and V. Ganesan, J. Phys. Chem. B **114**, 8367 (2010).
[43] H. Abroshan, H. Akbarzadeh, F. Taherkhani and G.A. Parsafar, Mol. Phys. **108**, 3393 (2010).
[44] M.J. Frisch, G.W. Trucks, H.B. Schlegel, G.E. Scuseria, M.A. Robb, J.R. Cheeseman, J.A. Montgomery Jr, T. Vreven, K.N. Kudin, J.C. Burant, J.M. Millam, S.S. Iyengar, J. Tomasi, V. Barone, B. Mennucci, M. Cossi, G. Scalmani, N. Rega, G.A. Petersson, H. Nakatsuji, M. Hada, M. Ehara, K. Toyota, R. Fukuda, J. Hasegawa, M. Ishida, T. Nakajima, Y. Honda, O. Kilao, H. Nakai, M. Klene, X. Li, J.E. Knox, H.P. Hratchian, J.B. Cross, C. Adamo, J. Jaramillo, R. Gomperts, R.E. Stratmann, O. Yazyev, A.J. Austin, R. Cammi, C. Pomelli, J.W. Ochterski, P.Y. Ayala, K. Morokuma, G.A. Voth, P. Salvador, J.J. Dannenberg, V.G. Zakrzewski, S. Dapprich, A.D. Daniels, M.C. Strain, O. Farkas, D.K. Malick, A.D. Rabuck, K. Raghavachari, J.B. Foresmnn, J.V. Ortiz, Q. Cui, A.G. Baboul, S. Clifford, J. Cioslowski, B.B. Stefanov, G. Liu, A. Liashenko, P. Piskorz, I. Komaromi, R.L. Martin, D.J. Fox, T. Keith, M.A. Al-Laham, C.Y. Peng, A. Nanayakkara, M. Challacombe, P.M.W. Gill, B. Johnson, W. Chen, M.W. Wong, C. Gonzalez and J.A. Pople, *GAUSSIAN 03. rev B.2* (Gaussian, Inc., Pittsburgh, PA, 2003).
[45] W.L. Jorgensen, J. Chandrasekhar, M.L. Madura and J.D. Klein, J. Chem. Phys. **79**, 926 (1983).
[46] W. Humphrey, A. Dalke and K. Schulten, J. Mol. Graphics **14**, 33 (1996).
[47] T. Takamatsu and A. Eisenberg, J. Appl. Polym. Sci. **24**, 2221 (1979).

[48] D.R. Morris and X. Sun, J. Appl. Polym. Sci. **50**, 1445 (1993).
[49] J.C. Phillips, R. Braun, W. Wang, J. Gumbart, E. Tajkhorshid, E. Villa, C. Chipot, R.D. Skeel, L. Kale and K. Schulten, J. Comput. Chem. **26**, 1781 (2005).
[50] S.E. Feller, Y.H. Zhang, R.W. Pastor and B.R. Brooks, J. Chem. Phys. **103**, 4613 (1995).
[51] J. Wang, P. Cieplak and P.A. Kollman, J. Comput. Chem. **21**, 1049 (2000).
[52] J. Wang, R.M. Wolf, J.W. Caldwell, P.A. Kollman and D.A. Case, J. Comput. Chem. **25**, 1157 (2004).
[53] A. Venkatnathan, R. Devanathan and M. Dupuis, J. Phys. Chem. B **111**, 7234 (2007).
[54] K. Vanommeslaeghe, E. Hatcher, C. Acharya, S. Kundu, S. Zhong, J. Shim, E. Darian, O. Guvench, P. Lopes, I. Vorobyov and A.D. MacKerell Jr, J. Comput. Chem. **31**, 671 (2010).
[55] I. Kusaka, Z.-G. Wang and J.H. Seinfeld, J. Chem. Phys. **108**, 6829 (1998).
[56] A.N. Isaev, J. Phys. Chem. A **114**, 2201 (2010).
[57] T. Darden, D. York and L. Pedersen, J. Chem. Phys. **98**, 10089 (1993).
[58] E.M. Lee, R.K. Thomas, A.N. Burgess, D.J. Barnes, A.K. Soper and A.R. Rennie, Macromolecules **25**, 3106 (1992).
[59] A. Hoffmann, J.-U Sommer and A. Blumen, J. Chem. Phys. **107**, 7559 (1997).
[60] A. Hoffmann, J.-U Sommer and A. Blumen, J. Chem. Phys. **106**, 6709 (1997).
[61] W.H. Joa and S.S. Jang, J. Chem. Phys. **111**, 1712 (1999).
[62] M. Fujimura, T. Hashimoto and H. Kawai, Macromolecules **14**, 1309 (1981).
[63] M. Fujimura, T. Hashimoto and H. Kawai, Macromolecules **15**, 136 (1982).
[64] M.D. Heaney and J. Pellegrino, Membr. Sci. **47**, 143 (1989).
[65] P.J. James, J.A. Elliott, T.J. McMaster, J.M. Newton, A.M.S. Elliott, S. Hanna and M.J. Miles, J. Mater. Sci. **35**, 5111 (2000).
[66] A. Lehmani, S. Durand-Vidal and P.J. Turo, Appl. Polym. Sci. **68**, 503 (1998).
[67] A.L. Rollet, O. Diat and G. Gebel, J. Phys. Chem. B **106**, 3033 (2002).
[68] Z. Porat, J.R. Fryer, M. Huxham and I. Rubinstein, J. Phys. Chem. **99**, 4667 (1995).
[69] S. Schlick and M.G. Alonso-Amigo, Macromolecules **22**, 2634 (1989).
[70] S. Schlick, M.G. Alonso-Amigo and J. Bednarek, Colloids Surf. A **72**, 1 (1993).
[71] M.J. Fricsh, J.A. Pople and J.S. Binkley, J. Chem. Phys. **80**, 3265 (1984).
[72] A.D. Becke, J. Chem. Phys. **98**, 5648 (1993).
[73] C. Lee, W. Yang and R.G. Parr, Phys. Rev. B **37**, 785 (1988).
[74] R.A. Kendall, T.H. Dunning Jr and R.J. Harrison, J. Chem. Phys. **96**, 6796 (1992).
[75] D.E. Woon and T.H. Dunning Jr, J. Chem. Phys. **98**, 1358 (1993).
[76] S. Urata, J. Irisawa, A. Takada, S. Tsuzuki, W. Shinoda and M. Mikami, Phys. Chem. Chem. Phys. **6**, 3325 (2004).
[77] L. Dougan, S.P. Bates, R. Hargreaves, J.P. Fox, J. Crain, J.L. Finney, V. Réat and A.K. Soper, J. Chem. Phys. **121**, 6456 (2004).
[78] Y. Zhong, G. Lee Warren and S. Patel, J. Comput. Chem. **29**, 1142 (2008).
[79] H. Yu, D.P. Geerke, H. Liu and W.F. Van Gunsteren, J. Comput. Chem. **27**, 1494 (2006).
[80] M. Saito, S. Ikesaka, J. Kuwano, J. Qiao, S. Tsuzuki, K. Hayamizu and T. Okada, Solid State Ionics **178**, 539 (2007).
[81] N. Agmon, Chem. Phys. Lett. **244**, 457 (1995).
[82] J.A. Morrone, K.E. Haslinger and M.E. Tuckerman, J. Phys. Chem. B **110**, 3712 (2006).
[83] T. Yergovich, G. Swift and F. Kurata, J. Chem. Eng. Data **16**, 222 (1971).
[84] R. Gibson, J. Chem. Phys. **57**, 1551 (1935).
[85] R. Lama and B.C-Y. Lu, J. Chem. Eng. Data **10**, 216 (1965).
[86] H. Schott, J. Chem. Eng. Data **14**, 236 (1969).
[87] W.S. Price, H. Ide and Y. Arata, J. Phys. Chem. A **103**, 448 (1999).
[88] G. Thau-Alexandrowicz, J. Membr. Sci. **4**, 151 (1978).
[89] P. Mark and L. Nilsson, J. Phys. Chem. A **105**, 9954 (2001).
[90] N.P. Blake, G. Mills and H. Metiu, J. Phys. Chem. B **111**, 2490 (2007).
[91] M.W. Verbrugge and R.F. Hill, J. Electrochem. Soc. **137**, 3770 (1990).
[92] I.M.J.J. Van De Ven-Lucassen, T.J.H. Vlugt, A.J.J. Van Der Zanden and P.J.A.M. Kerkhof, Mol Simulation **23**, 79 (1999).
[93] X. Ren, T.E. Springer, T.A. Zawodzinski and S. Gottesfeld, J. Electrochem. Soc. **147**, 466 (2000).
[94] D.T. Hallinan Jr and Y.A. Elabd, J. Phys. Chem. B **111**, 13221 (2007).